# Expression profile of SYNE3 and bioinformatic analysis of its prognostic value and functions in tumors

**Liwei Liao**
Department of Radiation Oncology, Nanfang Hospital, Southern Medical University, Guangzhou, Guangdong, China

**Longshan Zhang**
Department of Radiation Oncology, Nanfang Hospital, Southern Medical University, Guangzhou, Guangdong, China

**Mi Yang**
Department of Radiation Oncology, Nanfang Hospital, Southern Medical University, Guangzhou, Guangdong, China

**Xiaoqing Wang**
Department of Radiation Oncology, Nanfang Hospital, Southern Medical University, Guangzhou, Guangdong, China

**Weiqiang Huang**
Department of Radiation Oncology, Nanfang Hospital, Southern Medical University, Guangzhou, Guangdong, China

**Xixi Wu**
Department of Radiation Oncology, Nanfang Hospital, Southern Medical University, Guangzhou, Guangdong, China

**Hua Pan**
Department of Radiation Oncology, Nanfang Hospital, Southern Medical University, Guangzhou, Guangdong, China

**Lu Yuan**
Chronic Airways Diseases Laboratory, Department of Respiratory and Critical Care Medicine, Nanfang Hospital, Southern Medical University, Guangzhou, Guangdong, China

**Wenqi Huang**
Chronic Airways Diseases Laboratory, Department of Respiratory and Critical Care Medicine, Nanfang Hospital, Southern Medical University, Guangzhou, Guangdong, China

**Yuting Wu**
Chronic Airways Diseases Laboratory, Department of Respiratory and Critical Care Medicine, Nanfang Hospital, Southern Medical University, Guangzhou, Guangdong, China

**Jian Guan** ( guanjian5461@163.com )

**Research**

**Keywords:** SYNE3, expression profile, ceRNA network, immune infiltrition, bioinformatic analysis, tumor

**Posted Date:** March 13th, 2020

**DOI:** https://doi.org/10.21203/rs.3.rs-17159/v1



**Version of Record:** A version of this preprint was published on September 18th, 2020. See the published version at https://doi.org/10.1186/s12967-020-02521-7.

# Abstract

Background: Spectrin repeat containing nuclear envelope family member 3 (SYNE3) encodes an important component of linker of cytoskeleton and nucleoskeleton (LINC) complex, namely nesprin-3. In tumor, invasiveness and metastasis rely on the integrity of LINC complex, while the role of SYNE3/nesprin-3 in cancer is rarely studied.

Methods: Here, we explored the expression pattern, prognostic value and related mechanisms of SYNE3 through both experimental and bioinformatic methods. We first detected SYNE3 in BALB/c mice, normal human tissues and the paired tumor tissues, then used bioinformatic databases to verify our results. We further analyzed the prognostic value of SYNE3. Next, we predicted miRNA targeting SYNE3 and built a competing endogenous RNA (ceRNA) network and a transcriptional network by analyzing data from the cancer genome atlas (TCGA) database. Interacting genes of SYNE3 were predicted, and we further performed GO and KEGG enrichment analysis on these genes. Besides, the relationship of SYNE3 and immune infiltration was also investigated.

Results: SYNE3 exhibited various expressions in different tissues, mainly located on nuclear and in cytoplasm sometimes. SYNE3 expression level had prognostic value in tumors, possibly by stablizing nucleus, promoting tumor cells apoptosis and altering tumor microenvironment. Additionally, we constructed a RP11-2B6.2-miR-149-5p-/LINC01094-miR-330-3p-SYNE3 ceRNA network and a SATB1-miR-149-5p-SYNE3 transcriptional network in lung squamous cell carcinoma to support the tumor-suppressing role of SYNE3.

Conclusions: Our study explored novel anti-tumor functions and mechanisms of SYNE3, which might be useful for future cancer therapy.


# Background

Malignant tumor has unique biological characteristics such as abnormal cell differentiation and proliferation, loss of growth control, invasiveness and metastasis, making tumors easy to recur, metastasize or spread. Moreover, all these processes need morphological change of cells, which rely highly on the cytoskeleton remodeling. In this way, maintenance and regulation of cytoskeleton are vital in cancer development.

Cytoskeleton is an interactive protein network placed among cytoplasm, consisting of microtubule, microfilament and intermediate filament. Inside the nucleus, there is another similar structure known as nucleoskeleton, with a closer relationship with chromosomes, genes and nucleus.

Though specially divided by nuclear membrane, cytoskeleton and nucleoskeleton are functionally related. This point was strongly supported by the discovery of linker of nucleoskeleton and cytoskeleton (LINC) complex on nuclear membrane. LINC connects nucleoskeleton and cytoskeleton structurally and

functionally. Furthermore, the integrity of LINC was a significant precondition for functional cytoskeleton and nucleoskeleton.

Hence, understanding LINC is worthy of better recognizing the mechanisms of cell activities and tumor progressing. Therefore, as a crucial component of LINC, Nesprin (Nuclear envelope spectrin repeat protein) is getting increasing attention since it was originally discovered. Nesprins are a set of evolutionarily-conserved structural proteins, widely-expressed in vertebrate cells. Located on nuclear membrane, nesprins connect cytoskeleton to nucleus and engage in maintenance and adjustment of cytoskeleton. There are 4 discovered nesprin members. Nesprin-1 and nesprin-2 are two giant members most early recognized, sharing similar structures and functions. They can directly connect to microtubules and microfilaments, thus indirectly links to various cellular organelles. Nesprin-1/2 actively participate in mechanics transition, cellular organelles adjustment, cell migration, etc. Experiments suggested that lack or dysfunction of nesprin-1/2 led to muscular or central nervous system disorders [1]. Besides, nesprin-1/2 also engages in tumor metastasis [2, 3]. Unlike nesprin-1/2, nesprin-3/4 can only indirectly bind to microtubules with their corresponding binding partners [4]. Moreover, nesprin-3 can uniquely link to intermediate filament as well [5]. Similarly, nesprin-3/4 were also involved in nucleus migration and cell polarization. As for related diseases, mutated nesprin-4 was reported to correlate with progressive high-frequency hearing loss [6, 7]. Surprisingly, though having unique bond with IF and actively participating in cell differentiation, dysfunction or knocking-out of nesprin-3 seems to cause few changes on phenotypes. Even so, recent studies began to focus on its roles in cancer, mostly on how nesprin-3 mediates tumor cell migration [8, 9].

In this study, we tried to have a basic analysis of spectrin repeat containing nuclear envelope family member 3 (SYNE3), the coding gene of nesprin-3, in both experimental and bioinformatic aspects. Firstly, expression profile and histological distribution of SYNE3 in various BALB/c mice tissues, human normal tissues and paired tumor tissues were displayed. For its potential roles in cancer, the prognostic value of SYNE3 was discussed in patients with tumor. Additionally, SYNE3 and its interacting genes were listed and their functions were analyzed. At last, we investigated how SYNE3 expression affected tumor immune infiltration, thus influencing prognosis.

## Methods

# Specimen collection

We collected 12 types of normal tissues from 4-week-old BALB/C mice, which were purchased from the Experimental Animal Center of Southern Medical University, including tissues from gut, lung, liver, thyroid, brain, spleen, trachea, kidney, esophagus, stomach, heart and pancreas. The investigation conforms with the Guide for the Care and Use of Laboratory Animals published by the US National Institutes of Health (NIH Publication No. 85 – 23, revised 1996).

We also collected 9 specimen of resected tumor tissues and paired normal tissues from patients with cancer undergoing surgical resection in Nanfang hospital during 2019-1 to 2019-10, including tumors from liver, cervix, colon, small intestine, kidney, esophagus, breast and 2 cancer types from lung. Informed consent was obtained from each patient on the day of admission. The study protocol conforms to the ethical guidelines of the World Medical Association, Declaration of Helsinki Ethical Principles for Medical Research Involving Human Subjects adopted by the 18th WMA General Assembly, Helsinki, Finland, June 1964, as revised in Tokyo 2004. All patients have received no anti-tumor treatments before their surgeries, including radiotherapy, chemotherapy, biological immunotherapy and multiple operations. Over 80% tumor cells were contained in each cancer specimen, as certified by microscopic observation.

# Immunohistochemistry (IHC)

Collected tissues were fixed in 4% paraformaldehyde, dehydrated, then embedded in paraffifin and sliced into sections of 4 μm thickness. The sections were baked in oven at 65 ℃ for 1.5 hours and then hydrated. Next, antigen retrieval was practiced in boiling Tris/EDTA buffer (pH 9.0) at 100℃ for 12 minutes, then followed by incubation in 3% superoxol for 15 min to block endogenous peroxidase. The tissues were incubated with anti-SYNE3 monoclonal antibody diluted 25-fold (Thermo Fisher Scientific, USA) for incubation at 4 °C overnight. Then anti-rabbit secondary antibody (ORIGENE) was added and incubated at room temperature for 1 h. Next, diaminobenzidine (DAB) was used to reveal the color of antibody staining. Finally, the slides were mounted and observed under an optical microscope (Leica, Germany).

# Bioinformatics mining of SYNE3

We acquired the chromosome localization of SYNE3 on GeneCards database (https://www.genecards.org/). SYNE3 gene structure was analyzed on Ensembl database (http://asia.ensembl.org/), with its protein structure analyzed in Uniprot database (https://www.uniprot.org/), then visualized by using Illustrator for biological sequences software (IBS, http://ibs. biocuckoo.org/). we further accessed transcripts of SYNE family from Uniprot and constructed a phylogenetic tree by using MAFFT (https://mafft.cbrc.jp/alignment/server/) and ITOL (https://itol.embl.de/gallery.cgi). The protein-sequence comparison among different species was analyzed by utilizing DNAMAN software (lynnonBiosoft, USA).

Transcriptome data of diverse tumor tissues and their precancerous tissue were downloaded from The Cancer Genome Atlas (TCGA) (https://portal.gdc.cancer.gov/) database. Expression results in normal tissue were analyzed by utilizing University of California, Santa Cruz (UCSC) Xena browser (https://xenabrowser.net). Expression pattern, Disease-free survival (DFS) analysis and overall survival (OS) analysis of SYNE3 in 33 cancer types were performed on gene expression profiling and interactive analyses (GEPIA) database (http://gepia.cancer-pku.cn/).

MiRNAs targeting SYNE3 were predicted based on four different databases (DIANA-TarBase v8, miRWalk, TargetScanHuman and mirDIP). Furthermore, lncRNA-miRNA relationships of predicted SYNE3-associated miRNAs were obtained by overlapping results from starBase (http://starbase.sysu.edu.cn/)

and DIANA-LncBase v2 (http://carolina.imis.athena-innovation.gr/diana_tools/web/index.php?r=lncbasev2%2Findex-predicted). The overlapping result was pictured by website Bioinformatics & Evolutionary Genomics (http://bioinformatics.psb.ugent.be/webtools/Venn/). Finally, a competitive endogenous RNA (ceRNA) network regulating SYNE3 was constructed by using Cytoscape (version 3.6.0, http://www. cytoscape.org/).

We screened interacting genes of SYNE3 from STRING (Search Tool for the Retrieval of Interacting Genes) database (http://string-db.org) with a confidence score of $\geq 0.4$ was eligible for protein-protein interactions network (PPI) network construction and used Cytoscape to adjust it.

We performed gene ontology (GO) enrichment analysis on 41 interactive genes of SYNE3 by online Database for Annotation, Visualization and Integrated Discovery (DAVID; https://david.ncifcrf.gov/summary.jsp), and then the results of biological process (BP), cellular component (CC), molecular function (MF) were accessed to explore their functions. Moreover, Kyoto Encyclopedia of Genes and Genomes (KEGG) pathway of those 41 genes was analyzed in KOBAS 3.0 (http://kobas.cbi.pku.edu.cn/). Then, website imageGP (http://www.ehbio.com/ImageGP/) was utilized to make GO enrichment plot and KEGG plot. Simultaneously, the most enriched pathway was visualized by using KEGG Mapper, a collection of tools for KEGG mapping, with enriched genes marked in orange.

Tumor IMmune Estimation Resource (TIMER; https://cistrome.shinyapps.io/timer/) database was used to investigate how SYNE3 expression influenced tumor microenvironment, and the connection of different immune infiltration levels and corresponding prognosis. Gene Set Enrichment Analysis (GSEA) was performed using software GSEA v4.0.3 Java Web Start using gene set C7: immunologic signatures gene sets acquired from Molecular Signatures Database (MsigDB). Moreover, the correlation between SYNE3 and immune-cell markers was analyzed by GEPIA.

## Statistical analysis

All our data were analyzed on software GraphPad Prism (version 6.02, San Diego, California, USA). We applied Student's t-test to compare two different groups, and used Pearson correlation method for correlation analysis of SYNE3. $P < 0.05$ was considered statistically significant and false discover rate (FDR) < 0.05 was regarded statistically credible. The strength of the correlation was determined using the following guide for the correlative value: 0.00–0.19 "not related," 0.20–0.39 "weak," 0.40–0.59 "moderate," 0.60–0.79 "strong," 0.80–1.0 "very strong."

# Results

## Structure and dendrogram of SYNE3

SYNE3 located at 14q32.13, containing 18 exons and 17 introns (Fig. 1a). SYNE3 encoded 2 isoforms, nesprin-3α and nesprin-3β. Nesprin-3α was the dominant isoform and the main undertaker of nesprin-3 functions. The protein structure of nesprin-3α consisted of two parts of spectrin repeats, a KASH domain

and a coiled coil region (Fig. 1b). To study the conservation of SYNE3 among distinct species, we compared protein sequences encoded by SYNE3 among 6 different species (Fig. 1d), showing that Homo sapiens SYNE3 shared 77, 30, 78, 77 and 79% identity to Mus musculus, Danio rerio (zebrafish), Oryctolagus cuniculus, Rattus norvegicus and Ovis aries, respectively. It presented that SYNE3 was highly conserved in mammals, but varied greatly between human and zebrafish, a common animal model to study SYNE3 functions in neurons and stem cells. Moreover, a phylogenetic tree was constructed to analyze the conservative relationship among SYNE family members (Fig. 1c). In this tree, SYNE family was divided into two main clusters, one included two SYNE2 isoforms and the other contained the other SYNEs. More specifically, SYNE3, SYNE1 and the left SYNE2 isoforms were in the same subset, while SYNE4 was not.

# Expression of SYNE3 in BALB/c mice tissues

As BALB/c mice was a widely-used animal model in studies on tumorigenesis and tumor migration, we first detected the SYNE3 expression of various normal tissues in BALB/c mice (Fig. 2a). SYNE3 staining was positive in gut, lung, trachea, esophagus, stomach and heart, while not obvious in liver, thyroid, brain, spleen, kidney and pancreas. In gut, weak positive staining of SYNE3 was found in cytoplasm of intestinal villi and gland. The lung presented moderate staining in nucleus of epithelial cells. SYNE3 was strongly detected in nucleus in all layers of trachea, and moderate in cytoplasm in mucosal layer. For esophagus, nucleus staining was strong in all layers and cytoplasmic staining was moderate in all layers except submucosal cells. In stomach, weak staining was observed in cytoplasm of chief cells and parietal cells. In heart, only the nucleus of cardiomyocytes exhibited weak staining.

# Expression of SYNE3 in normal tissues and tumor tissues of human

We carried out IHC on samples of eight types of human normal tissues and their corresponding tumor tissues (Fig. 2b). In liver, only the cancer cells presented weak SYNE3 staining in cytoplasm. No SYNE3 was detected in both the normal and tumor cervix tissues. Weak positive staining was found in cytoplasm of normal gut epithelial cells, compared with moderate positive staining in cytoplasm of colon adenocarcinoma cells. Both small intestine and esophagus showed no staining in normal tissue and weak staining in their cancer cells. In terms of the kidney, moderate to strong positive staining was presented in both nucleus and cytoplasm of normal renal tubular epithelial cells, while only weak staining was found in whole cells of renal clear cell carcinoma. Breast and lung presented the most obvious expression differences between the normal and the tumor tissues. In normal tissues, strong positive staining was observed in the nucleus and cytoplasm of breast luminal epithelial cells and the nucleus of lung alveolar epithelial cells. While in the corresponding tumor samples, SYNE3 staining was only weakly presented in cancer cells.

We also referred to UCSC database (Fig.S1a). Compared with our experimental data, SYNE3 mRNA was expressed most in breast and lung as well. It was contradictory that the SYNE3 mRNA level in kidney was

low, though our IHC result showed moderate to strong positive staining.

Meanwhile, according to GEPIA database, SYNE3 was significantly expressed less in 9 cancer types, including breast invasive carcinoma (BRCA), lung adenocarcinoma (LUAD) and lung squamous cell carcinoma (LUSC)($P < 0.0001$), which were consistent with our IHC results in these tumors. However, only in acute myeloid leukemia (LAML), SYNE3 expression level is higher in tumor tissue compared with normal one ($P < 0.0001$). The expression change in LAML is the most noticeable, with its fold change reaching 9.26 (Fig.S1b).

# Prognostic value of SYNE3

To discover cancer prognostic value of SYNE3, we investigated the connection between SYNE3 expression level and DFS of patients with cancer, finding that higher SYNE3 expression brought longer lifespan to patients with renal clear cell carcinoma (KIRC) ($P = 0.033$, $HR = 0.67$) or with cervical squamous cell carcinoma and endocervical adenocarcinoma (CESC) ($P = 0.046$, $HR = 0.56$) (Fig.S2a). In terms of analysis of OS, five out of 33 kinds of tumor showed significant results (Fig.S2b). Specifically, we found that in KIRC ($P < 0.001$, $HR = 0.58$, Kaplan-Meier), LUAD ($P = 0.011$, $HR = 0.67$), CESC ($P = 0.02$, $HR = 0.57$) and squamous cell carcinoma of head and neck (HNSC) ($P = 0.046$, $HR = 0.76$), patients with high SYNE3 expression survive longer than others with low SYNE3 expression level. However, the case was in reverse in brain lower grade glioma (LGG) ($P = 0.034$, $HR = 1.5$), which patients with higher SYNE3 expression live even shorter. These results suggested SYNE3 prognostic value in various cancer types.

# Construction of ceRNA network of SYNE3 in LUSC

We analyzed the upstream regulation of SYNE3, screening miRNAs or lncRNAs which targeted SYNE3. We found 37 miRNAs possibly targeting SYNE3 from DIANAmT database, 2289 from miRWalk database, 317 from TargetScan database and 45 from mirDIP database (Fig. 3a). As a result, we screened hsa-miR-330-3p and hsa-miR-149-5p as the most vital miRNA regulators by overlapping prediections of four databases. We also presented the complementary sequences between SYNE3 and miR-330-3p and miR-149-5p (Fig. 3e). Then, we predicted 8 lncRNAs that can bind with hsa-miR-330-3p and 19 lncRNAs targeting miR-149-5p. In this way, we constructed a lncRNA-miRNA-mRNA network (Fig. 3b), in which lncRNA competitively bound with miRNA and weakened the suppression from miRNA to SYNE3.

To verify this ceRNA network, we took LUSC as an example, for LUSC presented significant difference in SYNE3 expression between normal and tumor tissues, and previous studied have revealed SYNE3 connection with lung cancer development [8, 10]. SYNE3 expression (Fig. 3c), miRNAs expression (Fig. 3d) and expression of lncRNAs were compared between tumor tissues of LUSC and normal ones. SYNE3 expressed significantly lower in tumor tissues of LUSC and both two miRNAs expressed higher in tumor tissues instead. In terms of lncRNAs, RP11-2B6.2 and LINC01094 presented a significant decrease in their expression (Fig. 3f). Combining with these analyses and interactions predicted by database above (Fig. 3g), we might suppose that RP11-2B6.2 and LINC01094 bind with hsa-miR-149-5p and hsa-miR-330-3p respectively to weaken miRNA suppression toward SYNE3 in LUSC (Fig. 3h).

# Transcriptome Analysis on SYNE3 in LUSC

To better understand the upstream mechanisms of SYNE3, we continued to do some transcriptome analysis on SYNE3, still using the example of LUSC. First, we constructed a transcriptional regulatory network involving 100 transcriptional factors predicted by GCBI database (Fig. 4a). Then, we selected 21 TFs with significant expression differences in normal tissues and tumor tissues of LUSC (Fig. 4b). Among them, SATB1 was correlated with SYNE3 expression (Fig. 4c, $r = 0.395$, $P < 0.0001$). Combined with the analysis of ceRNA network above, we wondered if the predicted SYNE3-related miRNAs also participated in TF regulation. By using the data of Tarbase, mirDIP, miRWalk and our predicted results, we identified miR-149-5p as an upstream regulator of SATB1 (Fig. 4d). Moreover, in LUSC, SATB1 and SYNE3 were both downregulated while miR-149-5p was expressed more. Based on these, a SATB1-miR-149-5p-SYNE3 transcriptional network in LUSC was constructed (Fig. 4e).

# KEGG and GO pathway enrichment analysis of SYNE3

To investigate the downstream regulation of SYNE3, a PPI network (Fig. 5a) was built with 40 interacting genes of SYNE3 predicted by STRING database. We performed KEGG analysis of SYNE3 and its 40 interacting genes on KOBAS, and finally acquired 6 KEGG pathways these 41 genes were enriched in, specifically ribosome, apoptosis, arrhythmogenic right ventricular cardiomyopathy (ARVC), hypertrophic cardiomyopathy (HCM), dilated cardiomyopathy and p53 signaling pathway, with KEGG map of ribosome especially presented (Fig. 5b).

For GO enrichment analysis, SYNE3 and its interacting genes were significantly and credibly enriched in 12 BPs, 11 CCs and 3 MFs (Fig. 5c). These genes mainly encoded protein from LINC, cytoskeleton, nucleoskeleton and ribosome, likely participating in nucleus adjustment and transcription.

# Immune Infiltration Level analysis in cancer associated with SYNE3

Higher SYNE3 expression was linked to better clinical outcomes in our analysis, suggesting its tumor-suppressing functions. Here, we explore this function in the aspect of immunity. First, we screened cancer types whose immune infiltration was correlated with SYNE3 expression. Accordingly, we found that SYNE3 expression was significantly correlated with dendritic cell, neutrophil, CD4 + T cell, macrophage, CD8 + T cell and B cell in 30, 30, 27, 26, 25, 25 and 22 types of cancer respectively.

We then analyzed each cancer type and found 10 types of cancer with significant results in all immune cell types and purity. Especially, in HNSC, KIRC and LUAD, both OS and immune infiltration were positively correlative with SYNE3 expression (Fig. 6a). Among these three cancer types, the survival of LUAD presented a closer relationship with the level of immune cell infiltration (Fig. 6b), which was positively correlated with the infiltration of B cell and dendritic cell.

Hence, we tended to figure out the role of SYNE3 expression in the immune infiltration of LUAD. In LUAD, higher SYNE3 expression corresponded with better clinical outcome (Fig. 6c) and the expression of SYNE3 was significantly downregulated (Fig. 6d) overall. We performed GSEA analysis on 535 TCGA samples divided into high group (267 samples) and low group (268 samples) by expression level. The result revealed that pathways indicative of DC cell and B cell activation significantly correlated with SYNE3 expression (Fig. 6e). To further confirm this point, we also analyzed the relationship between SYNE3 and biomarkers of DC cell [11, 12] and B cell [11] (Fig. 6f), with all correlations significant.

# Discussion

As a linker protein of cytoskeleton and nucleoskeleton, SYNE3/nesprin-3 has been shown to play a vital role in 3D cell migration [13] and tumor cell movement [9] in previous studies. However, these researches too limited to reveal SYNE3 functions in tumor. Therefore, in our study, we hoped to provide some basic knowledge of SYNE3 and analyze its roles in cancer.

Based on our analysis, SYNE3 was conserved among mammals and its family members, suggesting some vital roles of SYNE3 to keep through evolution. Moreover, SYNE3 shared more similarities with SYNE1 and SYNE2 than SYNE4 in its structure and may in its functions as well.

We investigated SYNE3 expression in various tissues. In normal human tissues, SYNE3 was strongly detected in breast and lung, corresponding with the highest mRNA level in these two tissues. Moreover, the expression difference between normal and tumor tissues was most obvious in breast and lung as well in both IHC and GEPIA. However, conflicts also existed, for instance, kidney was of low mRNA but moderate to high SYNE3 staining. For one hand, our tissues were just randomly selected cases, so they cannot represent general conditions like data from UCSC or GEPIA. For another hand, the mRNA level was not always consistent with protein level, though there was no related study on SYNE3 expression. In addition, though SYNE3 had been reported to exist widely, its expression was not always high enough to be detected.

In our prognostic analysis, we found higher SYNE3 expression level associated with longer OS in patients with KIRC, LUAD, CESC or HNSC except LGG with negative correlation. In most cases, the expression of SYNE3 was also downregulated in tumor. Recent study showed that knockdown of SYNE3 led to DNA damage, genome organization loss, and transcriptional changes [14], and these events were closely related to tumorigenesis for this mechanism had been reported in SYNE1[15]. Therefore, SYNE3 participated in some anti-tumor events and there might be various mechanisms to adjust SYNE3 expression.

CeRNA is a conception firstly proposed in 2011[16]. In ceRNA network, non-coding RNA, likely lncRNA or circRNA, can competitively bind with miRNA, thereby weaken the repression from miRNA to mRNA. We identified hsa-miR-330-3p and hsa-miR-149-5p as key regulatory miRNAs of SYNE3. MiR-330-3p was a recognized cancer-promoting factor. It was reported that miR-330-3p can target the gene of program cell death 4 (PDCD4) to promote tumor [17]. MiR-330-3p is also related with metastasis and invasion of lung

cancer, and glutamate receptor 3 (GRIA3) [18] and human manganese superoxide dismutase 2 (hSOD2) [19] are its two target genes. Researches found miR-330-3p is correlated with bad prognosis in breast cancer as well [20], in which miR-330-3p can target Collagen and Calcium Binding EGF Domains 1 (CCBE1) to promote cancer metastasis [21]. Higher miR-330-3p led to lower OS in renal cell carcinoma (RCC), though miR-330-3p also presented some tumor-suppressing functions in RCC [22], suggesting that further studies were needed to explain this paradox. However, the function of miR-149-5p depends on specific tumor types. MiR-149-5p can help to disable the invasion and proliferation of medullary thyroid carcinoma cells [23] and suppress the development of non-small cell lung cancer [24] and hepatocellular carcinoma [25, 26]. Combined with our survival analysis, tumor-promoting functions of miRNAs displayed more obvious in KIRC, CESC, LUAD and HNSC. While for LGG, there might be other mechanisms related to its unique progressive features or micro-environment, causing a contrary result.

In our ceRNA network, NEAT1 and MIR503HG are tumor suppressors targeting both miR-330-3p and miR-149-5p. NEAT1 can be mediated by Tumor protein P53 (P53), a critical tumor suppressor, to suppress transformation and cancer initiation [27]. MIR503HG can target heterogeneous nuclear ribonucleoprotein A2/B1 (HNRNPA2B1) and NF-κB signaling pathway to inhibit migration of hepatocellular carcinoma [28]. Meanwhile, only a few of the rest lncRNAs have been reported, including both tumor suppressors and tumor enhancers. These results showed double regulations in this ceRNA network of SYNE3, and tumor-suppresing lncRNAs seem to role more dominantly.

As for PPI network of SYNE3, it was reasonable for SYNE3 to interact with Sad1 And UNC84 Domain Containing (SUN) family, a set of cytoskeleton linker proteins and the other SYNE members. The function of SYNE3 is correlated with these binding partners, which was supported by GO and KEGG analysis. Based on our analysis, SYNE3 is correlated with some tumorous processes. P53 and 3 interacting genes of SYNE3 were involved in P53 signaling pathway, including cyclin-dependent kinase 1 (CDK1), Caspase 8 (CASP8) and cyclin B1 (CCNB1). CDK1 can adjust the cell cycle [29], CASP8 is referred as an apoptosis regulator [30], and CCNB1 is vital for mitosis and proliferation [31]. Moreover, apoptosis, a pathway closely to P53, also enriched 5 SYNE3 interacting genes, involving CASP8 again, LMNA, CASP6, LMNB1 and LMNB2. Among them, downregulation of CASP6 induced suppression of the apoptosis of chronic myeloid leukemia cells [32]. LMNB1 and LMNB2 are coding genes for lamin B1 and lamin B2 respectively, which are nucleoskeleton components associated with cancer and aging [33]. Besides, 9 interacting genes of SYNE3 code ribosomal proteins, indicating a possible association with transcription. Based on these, SYNE3 may suppress cancer by promoting tumor apoptosis, which can be realized through adjustment of cell cycle, recruitment of immune cells and alteration of nucleoskeleton and ribosome.

We finally focused on SYNE3 and immune property of tumor microenvironment. SYNE3 showed good correlation with tumor immune infiltration, especially in LUAD, as its OS was most relevant with its tumor microenvironment, especially with B cell and DC cell. It has already been reported that B-cell infiltration correlated with good prognosis in LUAD [34]. Dendritic cell is responsible for antigen presentation to T- and B-cells and activation natural killer (NK) cells and can activate anti-tumor immunity [35]. Therefore, regulating the infiltration of B cell and DC cell can be an effective pathway for SYNE3 to influence the

survival of patients with LUAD. GSEA analysis also showed that higher SYNE3 expression relating to pathways enhancing B cell and DC cell. Furthermore, SYNE3 also significantly correlated with markers of B cell and DC cell. Therefore, we supposed that higher expression of SYNE3 helped with the production and collection of B cell and DC cell, so that SYNE3 altered tumor microenvironment and presented significant and reasonable prognostic value in LUAD.

# Conclusions

Overall, our study firstly provided an overview of SYNE3 expression in diverse normal and tumor tissues. Then, we tended to explore the prognostic value of SYNE3. Though previous researches revealed its role in mediating tumor metastasis, we found higher SYNE3 expression correlated with even better clinical outcome. We then analyzed tumor-suppressing functions of SYNE3, showing that SYNE3 might engage in apoptosis mediation of tumor cells. Moreover, SYNE3 expression can impact immune cell infiltration as well, adjusting the local anti-tumor immunity to be more active and effective. Our study revealed the unexpected anti-cancer functions of SYNE3, and provided a new perspective of SYNE family in tumors, though still lacking of experimental verification. In addition to tumor metastasis, the role of SYNE3 in apoptosis, maintenance of nuclear stability and tumor microenvironment regulation in cancer is more obvious, especially in lung cancer. These findings might suggest a potential biomarker for tumor prognosis and therapy.

# Abbreviations

SYNE3: Spectrin repeat containing nuclear envelope family member 3; CeRNA: competing endogenous RNA; TCGA: the cancer genome atlas; IHC: Immunohistochemistry ; DFS: Disease-free survival; OS: Overall survival; GO: Gene ontology; BP: Biological process; CC: Cellular component; MF: Molecular function; KEGG: Kyoto Encyclopedia of Genes and Genomes; GSEA: Gene Set Enrichment Analysis; FDR: False discover rate; LUAD: Lung adenocarcinoma; LUSC: Lung squamous cell carcinoma; DC: Dendritic

# Declarations

### Ethical approval and consent to participate

This study was ratified by the Ethics Committee of Nanfang Hospital of Southern Medical University. All participants offered written informed consent before surgery. The 4-week-old male BALB/c mice were purchased from the Experimental Animal Center of Southern Medical University. The study conforms to the provisions of the Declaration of Helsinki.

### Consent for publication

Not applicable.

### Availability of data and material

All the analysis data were accessed from TCGA database (https:// portal.gdc.cancer.gov/).

### Competing interests

The authors declare no competing interests.


### Funding

The study was supported by National Natural Science Foundation of China (NO. 81602685, 81672992); Clinical Research Startup Program of Southern Medical University by High-level University Construction Funding of Guangdong Provincial Department of Education (LC2019ZD008); Clinical Research Startup Program of Southern Medical University by High-level University Construction Funding of Guangdong Provincial Department of Education (2018CR021); Health & Medical Collaborative Innovation Project of Guangzhou City, China (201803040003); the Natural Science Foundation of Guangdong Province (NO. 2017A030313486); Guangzhou Science and Technology Plan Project (201707010025) and CAMS Innovation Fund for Medical Sciences (CIFMS, 2016-I2M-1-017 and 2017-I2M-B&R-13).


### Author's contributions

J. G contributed to the study design and draft revision. H.P, M.Y and X.X.W contributed to human specimen collection and mice and tissue preparation. W.Q.H (Weiqiang Huang), L.Y, W.Q.H (Wenqi Huang) and Y.T.W contributed to perform immunohistochemical assay. X.Q.W and M.Y contributed to data collection and interpretation of bioinformatics results. L.S.Z and L.W.L contributed to immunohistochemical assay, draft the manuscript and coordinate data collection and analysis.


### Acknowledgements

We thank State Key Laboratory of Oncology in Southern Medical University for providing experimental platform.


## References


1. Zhou C, Rao L, Warren DT, Shanahan CM, Zhang Q. Mouse models of nesprin-related diseases. Biochem Soc T. 2018;3(46):669-681.
2. Infante E, Castagnino A, Ferrari R, Monteiro P, Agüera-González S, Paul-Gilloteaux P, et al. LINC complex-Lis1 interplay controls MT1-MMP matrix digest-on-demand response for confined tumor cell migration. Nat Commun. 2018;1(9):2443.
3. Shah K, Patel S, Modi B, Shah F, Rawal R. Uncovering the potential of CD44v/SYNE1/miR34a axis in salivary fluids of oral cancer patients. J Oral Pathol Med. 2018;4(47):345-352.
4. Ketema M, Arnoud S. Nesprin-3: a versatile connector between the nucleus and the cytoskeleton. Biochem Soc T. 2011;6(39):1719-1724.

5. Wilhelmsen K, Litjens SHM, Kuikman I, Tshimbalanga N, Janssen H, van den Bout I, et al. Nesprin-3, a novel outer nuclear membrane protein, associates with the cytoskeletal linker protein plectin. J Cell Biol. 2005;5(171):799-810.
6. Horn HF, Brownstein Z, Lenz DR, Shivatzki S, Dror AA, Dagan-Rosenfeld O, et al. The LINC complex is essential for hearing. J Clin Invest. 2013;2(123):740-750.
7. Worman HJ, Segil N. Nucleocytoplasmic connections and deafness. J Clin Invest. 2013;2(123):553-555.
8. Ji Y, Jiang J, Huang L, Feng W, Zhang Z, Jin L, Xing X. Spermassociated antigen 4 (SPAG4) as a new cancer marker interacts with Nesprin3 to regulate cell migration in lung carcinoma. Oncol Rep. 2018;2(40):783-792.
9. Petrie RJ, Harlin HM, Korsak LI, Yamada KM. Activating the nuclear piston mechanism of 3D migration in tumor cells. J Cell Biol. 2017;1(216):93-100.
10. Harryman WL, Pond E, Singh P, Little AS, Eschbacher JM, Nagle RB, Cress AE. Laminin-binding integrin gene copy number alterations in distinct epithelial-type cancers. Am J Transl Res. 2016;2(8):940-954.
11. Becht E, Giraldo NA, Lacroix L, Buttard B, Elarouci N, Petitprez F, et al. Estimating the population abundance of tissue-infiltrating immune and stromal cell populations using gene expression. Genome Biol. 2016;1(17):218.
12. Pan JH, Zhou H, Cooper L, Huang JL, Zhu SB, Zhao XX, et al. LAYN Is a Prognostic Biomarker and Correlated With Immune Infiltrates in Gastric and Colon Cancers. Front Immunol. 2019; (10):6.
13. Petrie RJ, Koo H, Yamada KM. Generation of compartmentalized pressure by a nuclear piston governs cell motility in a 3D matrix. Science. 2014;6200(345):1062-1065.
14. Heffler J, Shah PP, Robison P, Phyo S, Veliz K, Uchida K, et al. A Balance Between Intermediate Filaments and Microtubules Maintains Nuclear Architecture in the Cardiomyocyte. Circ Res. 2019.
15. Sur I, Neumann S, Noegel AA. Nesprin-1 role in DNA damage response. Nucleus (Austin, Tex.). 2014;2(5):173-191.
16. Salmena L, Poliseno L, Tay Y, Kats L, Pandolfi PP. A ceRNA hypothesis: the Rosetta Stone of a hidden RNA language? Cell. 2011;3(146):353-358.
17. Meng H, Wang K, Chen X, Guan X, Hu L, Xiong G, et al. MicroRNA-330-3p functions as an oncogene in human esophageal cancer by targeting programmed cell death 4. Am J Cancer Res. 2015;3(5):1062-1075.
18. Wei CH, Wu G, Cai Q, Gao XC, Tong F, Zhou R, et al. MicroRNA-330-3p promotes cell invasion and metastasis in non-small cell lung cancer through GRIA3 by activating MAPK/ERK signaling pathway. J Hematol Oncol. 2017;1(10):125.
19. Shen L, Yi S, Huang L, Li S, Bai F, Lei S, et al. MiR-330-3p promotes lung cancer cells invasion, migration, and metastasis by directly targeting hSOD2b. Biotechnol Appl Biochem. 2019;1(66):21-32.

20. Wang H, Chen SH, Kong P, Zhang LY, Zhang LL, Zhang NQ, Gu H. Increased expression of miR-330-3p: a novel independent indicator of poor prognosis in human breast cancer. Eur Rev Med Pharmacol Sci. 2018;6(22):1726-1730.
21. Mesci A, Huang X, Taeb S, Jahangiri S, Kim Y, Fokas E, et al. Targeting of CCBE1 by miR-330-3p in human breast cancer promotes metastasis. Br J Cancer. 2017;10(116):1350-1357.
22. Jin L, Li Y, Liu J, Yang S, Gui Y, Mao X, et al. Tumor suppressor miR-149-5p is associated with cellular migration, proliferation and apoptosis in renal cell carcinoma. Mol Med Rep. 2016;6(13):5386-5392.
23. Ye X, Chen X. MiR-149-5p inhibits cell proliferation and invasion through targeting GIT1 in medullary thyroid carcinoma. Oncol Lett. 2019;1(17):372-378.
24. Liu L, Chen Y, Li Q, Duan P. LncRNA HNF1A-AS1 modulates non-small cell lung cancer progression by targeting miR-149-5p/Cdk6. J Cell Biochem. 2019.
25. Chen EB, Zhou ZJ, Xiao K, Zhu GQ, Yang Y, Wang B, et al. The miR-561-5p/CX3CL1 Signaling Axis Regulates Pulmonary Metastasis in Hepatocellular Carcinoma Involving CX3CR1(+) Natural Killer Cells Infiltration. Theranostics. 2019;16(9):4779-4794.
26. Rouas R, Merimi M, Najar M, El ZN, Fayyad-Kazan M, Berehab M, et al. Human CD8(+) CD25 (+) CD127 (low) regulatory T cells: microRNA signature and impact on TGF-beta and IL-10 expression. J Cell Physiol. 2019;10(234):17459-17472.
27. Mello SS, Sinow C, Raj N, Mazur PK, Bieging-Rolett K, Broz DK, et al. Neat1 is a p53-inducible lincRNA essential for transformation suppression. Genes Dev. 2017;11(31):1095-1108.
28. Wang H, Liang L, Dong Q, Huan L, He J, Li B, et al. Long noncoding RNA miR503HG, a prognostic indicator, inhibits tumor metastasis by regulating the HNRNPA2B1/NF-kappaB pathway in hepatocellular carcinoma. Theranostics. 2018;10(8):2814-2829.
29. Castedo M, Perfettini JL, Roumier T, Kroemer G. Cyclin-dependent kinase-1: linking apoptosis to cell cycle and mitotic catastrophe. Cell Death Differ. 2002;12(9):1287-1293.
30. Tummers B, Green DR. Caspase-8: regulating life and death. Immunol Rev. 2017;1(277):76-89.
31. Nakayama Y, Yamaguchi N. Role of cyclin B1 levels in DNA damage and DNA damage-induced senescence. Int Rev Cel Mol Bio. 2013305):303-337.
32. Nie ZY, Yao M, Yang Z, Yang L, Liu XJ, Yu J, et al. De-regulated STAT5A/miR-202-5p/USP15/Caspase-6 regulatory axis suppresses CML cell apoptosis and contributes to Imatinib resistance. J Exp Clin Canc Res. 2020;1(39):17.
33. Garvalov BK, Muhammad S, Dobreva G. Lamin B1 in cancer and aging. Aging. 2019;18(11):7336-7338.
34. Varn FS, Tafe LJ, Amos CI, Cheng C. Computational immune profiling in lung adenocarcinoma reveals reproducible prognostic associations with implications for immunotherapy. Oncoimmunology. 2018;6(7):e1431084.
35. Hansen M, Andersen MH. The role of dendritic cells in cancer. Semin Immunopathol. 2017;3(39):307-316.

# Supplementary Information

**Additional file 1: Figure S1.** Expression pattern of SYNE3 refer to database. **a** Expression profile of SYNE3 in normal tissues acquired from University of California, Santa Cruz (UCSC) database. **b** SYNE3 RNA Expression in both normal and tumor tissues of human accessed from Gene Expression Profiling Interaction Analysis (GEPIA) database.

**Additional file 2: Figure S2.** Prognostic analysis of SYNE3. **a** Two significant results (KIRC and CESC) of disease free survival analysis on SYNE3, performed on GEPIA. **b** Five significant results (KIRC, LUAD, CESC, HNSC and LGG) of disease free survival analysis on SYNE3, performed on GEPIA.

# Figures

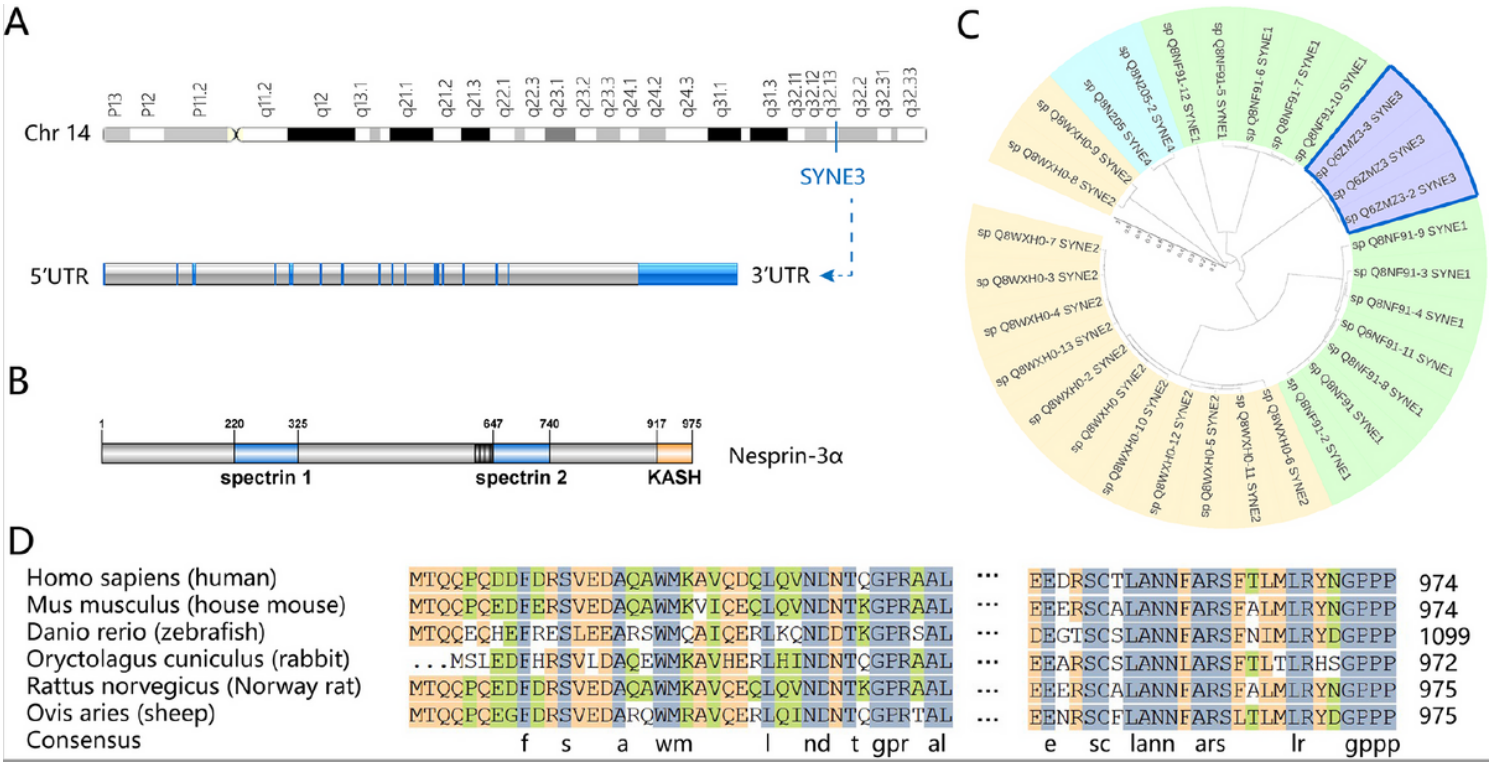


**Figure 1**

Gene structure, protein structure and conservative analysis of SYNE3. a Chromosome localization and gene structure of SYNE3 in human. b Structure of nesprin-3, the most common SYNE3 encoding protein. c phylogenetic tree of SYNE family. d Comparison of protein sequences encoded by SYNE3 among six different species.

**Figure 2**

Expression pattern of SYNE3 in BALB/c mice and human. a distribution of SYNE3 in tissues from BALB/c mice. b Immunohistochemistry results of SYNE3 performed in both normal and tumor tissues of human.

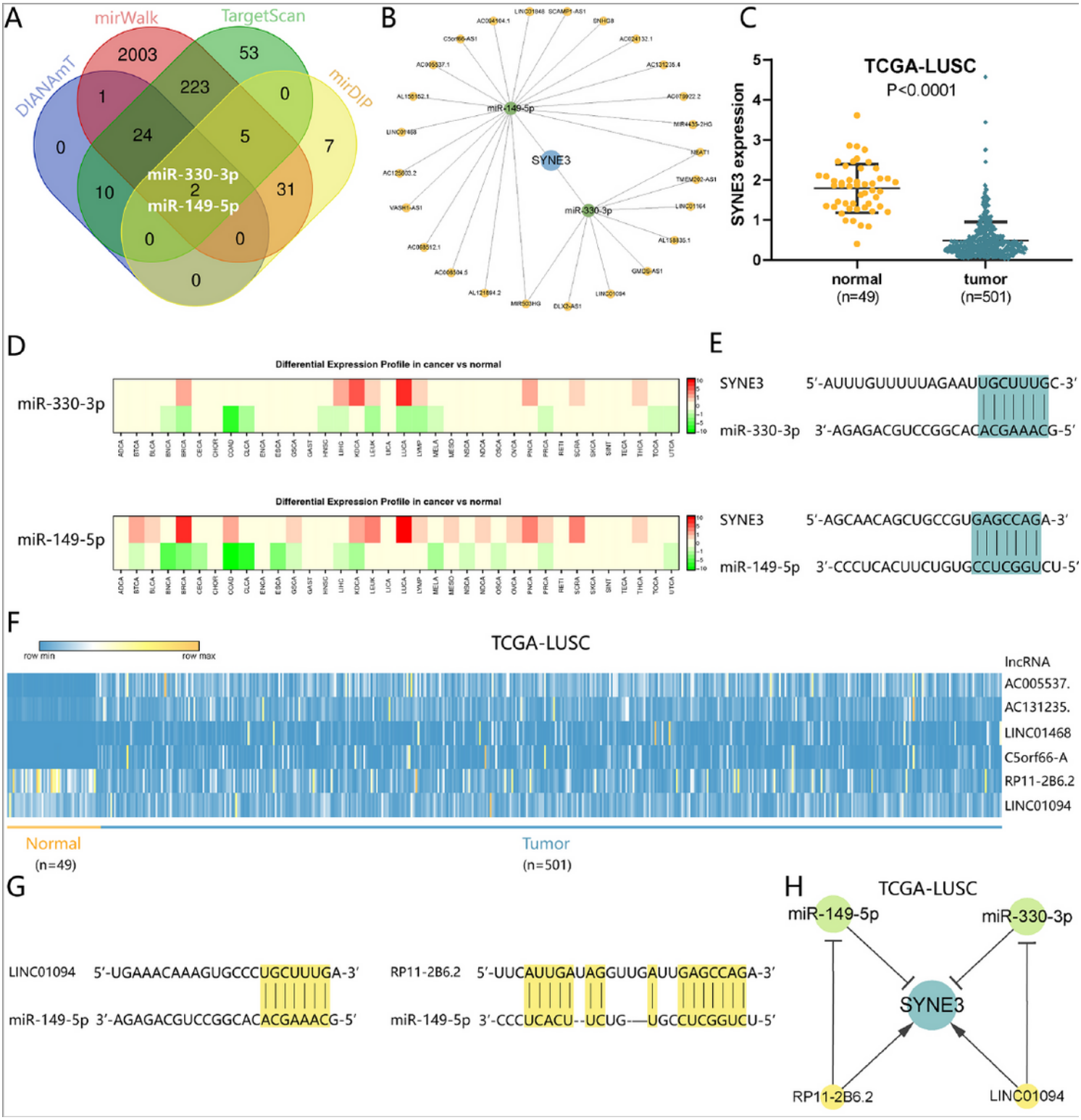


## Figure 3

Networks regulating SYNE3. a Result of predicted miRNAs using 4 different database, and hsa-miR-330-3p and hsa-miR-149-5p were finally screened by overlapping these data and the result was visualized on Bioinformatics & Evolutionary Genomics website. b Construction of ceRNA network of SYNE3. c SYNE3

expression in LUSC according to TCGA database. d differential expression profile in cancer vs normal of miR-330-3p and miR-149-5p. f lncRNAs in the network differently expressed in normal vs tumor in LUSC based on TCGA database. e, g predicted interaction between miR-149-5p and miR-330-3p and SYNE3, miR-149-5p and RP11-2B6.2 and LINC01094. h a ceRNA network in LUSC composed of SYNE3, miR-149-5p, miR-330-3p, RP11-2B6.2 and LINC01094.

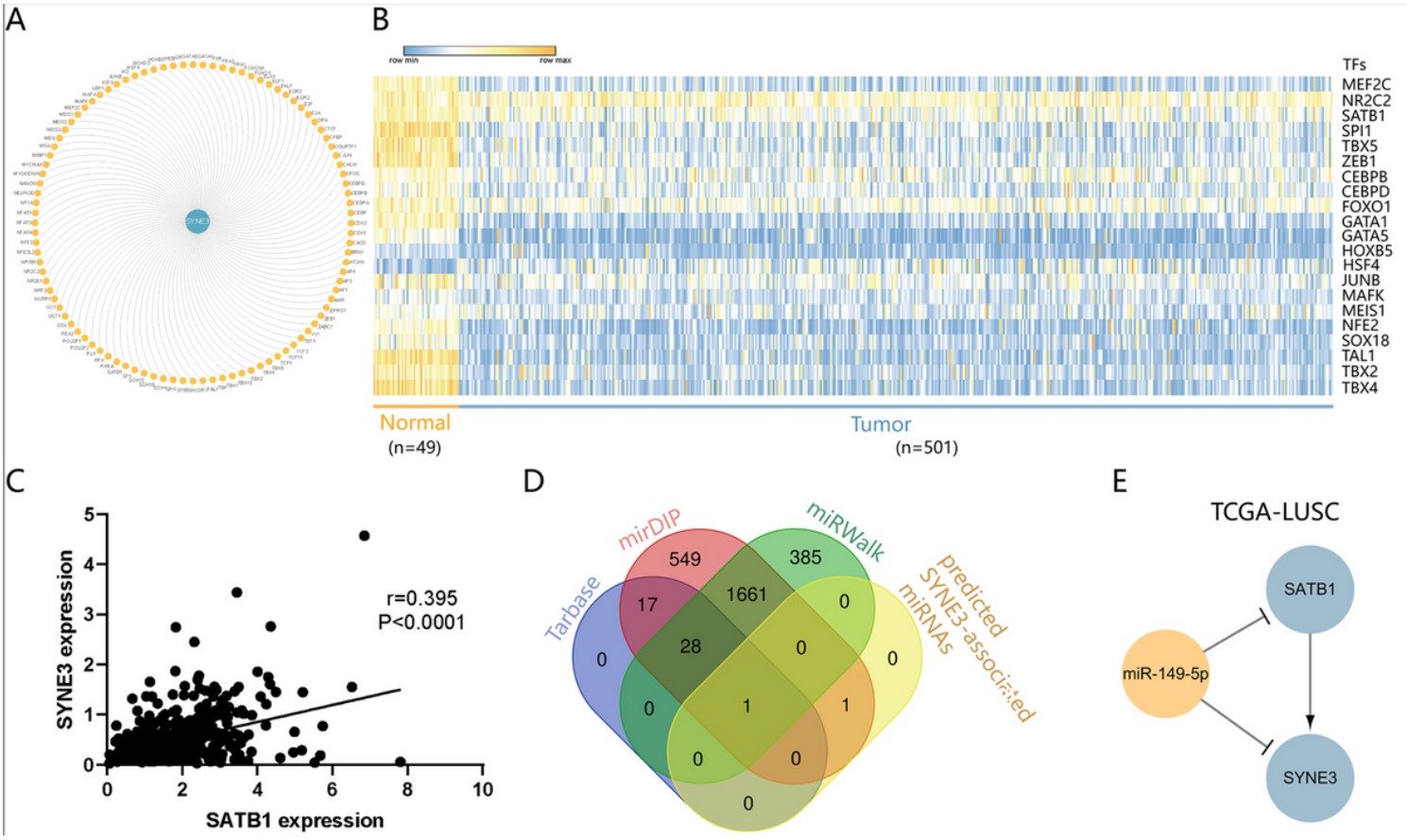


## Figure 4

Transcriptional network of SYNE3 in LUSC. a predicted SYNE3-associated transcriptional factors based on the results of GCBI online database. b TFs differently expressed in normal tissues and tumor tissues of LUSC. c Pearson correlation coefficient between SYNE3 expression and SATB1 expression. d miRNA screened to regulate SATB1, using the data of Tarbase, mirDIP, miRWalk and previous analysis. e transcriptional network among SYNE3, miR-149-5p and SATB1 in LUSC.

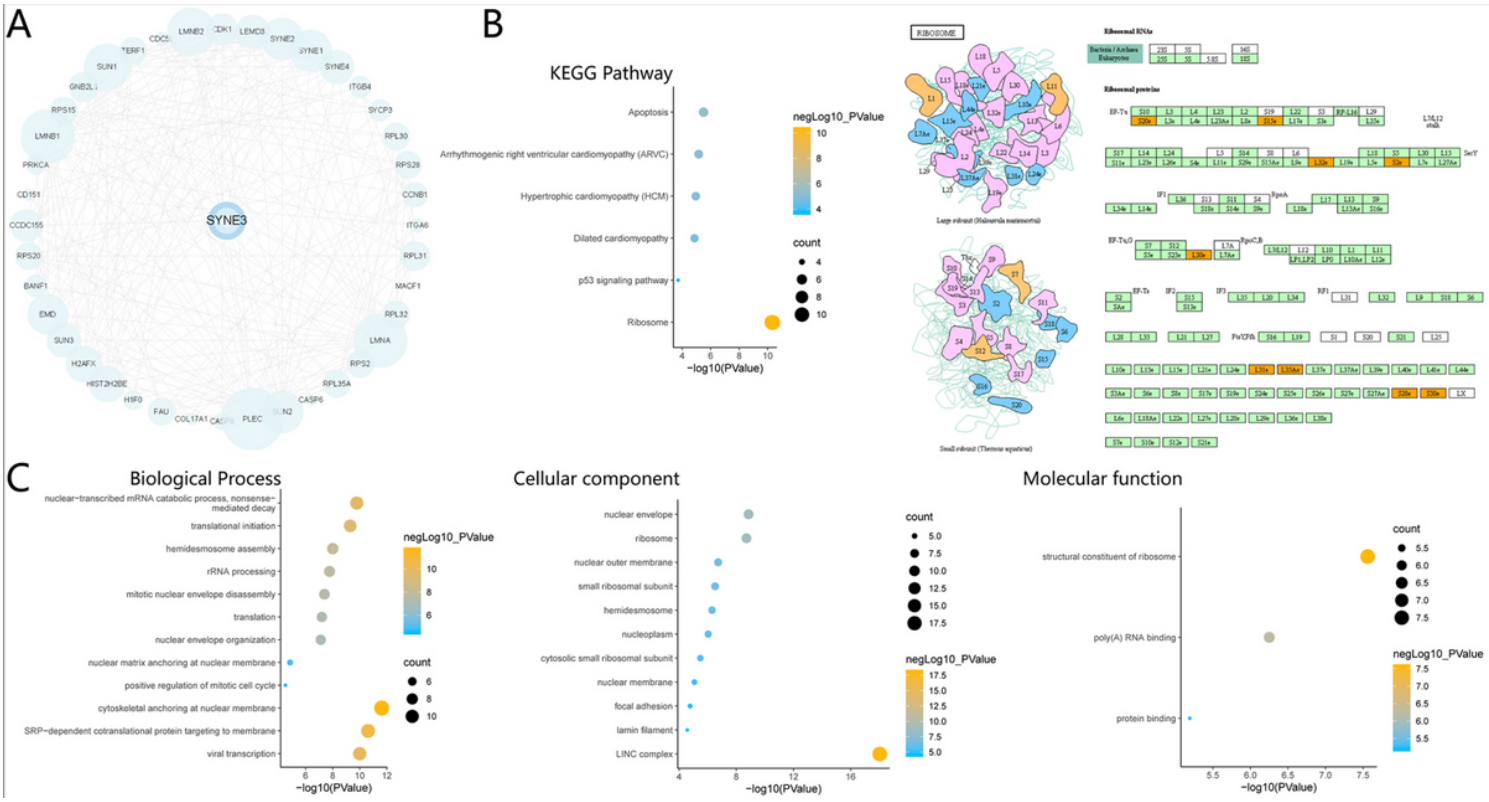


## Figure 5

Kyoto Encyclopedia of Genes and Genomes (KEGG) and Gene Ontology (GO) enrichment analysis of SYNE3. a an protein-protein interacting network of SYNE3 constructed with data from STRING. b KEGG enrichment was performed by using KOBAS 3.0 database, and the most enriched pathway map was pictured based on map from KEGG Mapper. c GO analysis was performed with DAVID (Database for Annotation, Visualization and Integrated Discovery) in three aspects: Molecular Function, Biological Process and Cellular Component.

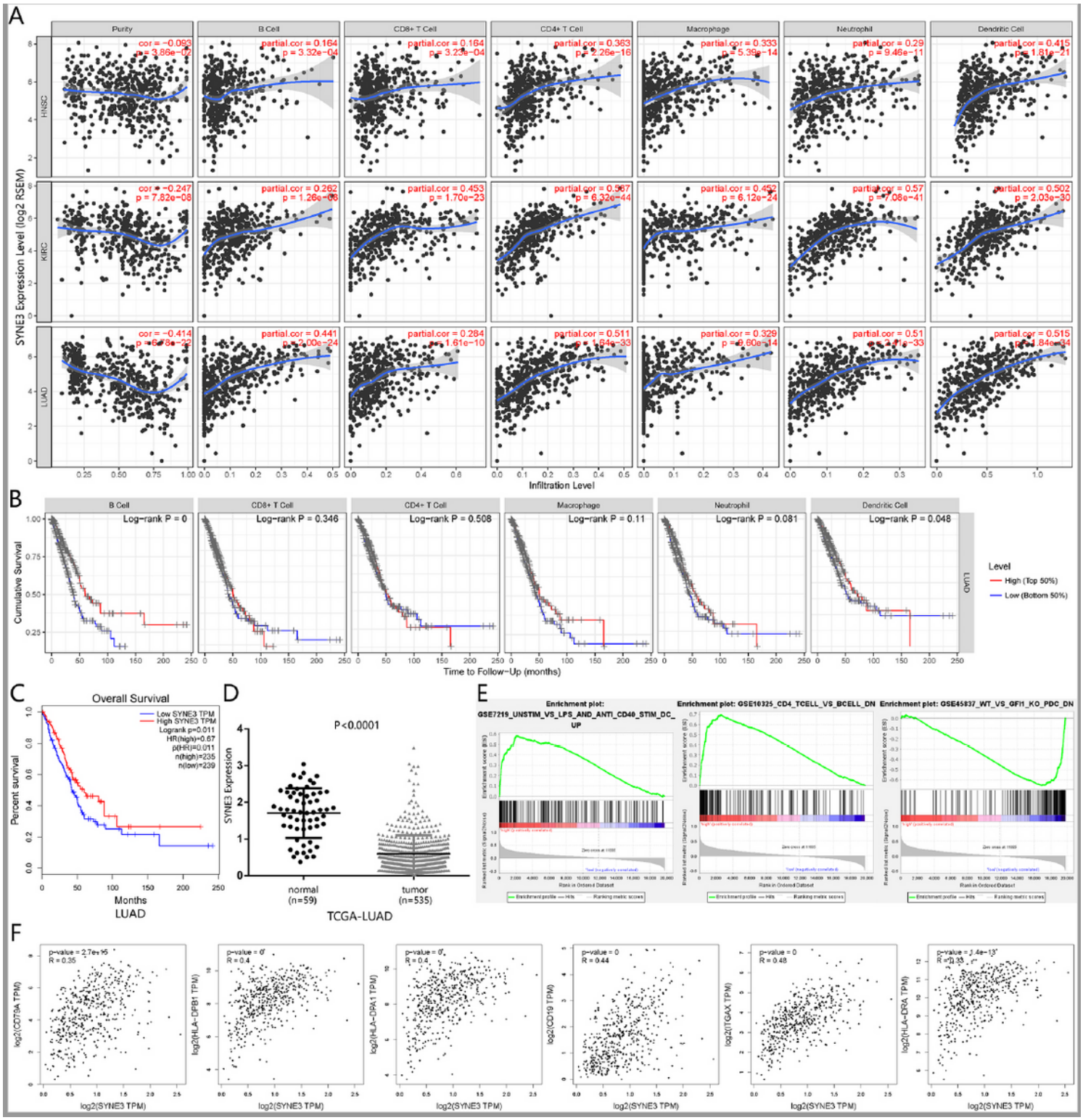


## Figure 6

The role SYNE3 played in tumor microenvironment. a Immune infiltration level associated with SYNE3 in HNSC, KIRC and LUAD analyzed in TIMER. b The relationship between immune cell infiltration and lung adenocarcinoma prognosis, higher infiltration level of B cell and dentritic cell were significantly associated with better clinical outcome of LUAD. c Higher SYNE3 expression was correlated with longer OS of patients with lung adenocarcinoma. d SYNE3 expression was significantly downregulated in LUAD

compared with that in normal lung tissues. e GSEA analysis grouped by SYNE3 expression level. f The correlation between SYNE3 expression and expression of B cell and dentritic cell based on GEPIA database.

## Supplementary Files

This is a list of supplementary files associated with this preprint. Click to download.

- FigureS2.pdf
- FigureS1.pdf